

Research Article | Volume 13, Issue 3 | Pages 572-579 | e-ISSN: 2347-470X

Unbalanced Voltage Enhancement based on STATCOM for Distribution Network Integrated with Renewable Energy

Waseem Kh. Ibrahim^{1 io}, Mahmood T. Alkhayyat^{2* io}, and Mohammed Y. Suliman³

¹University of Hamdaniya, Iraq; Email: waseem-kh82@uohamdaniya.edu.iq

ABSTRACT- STATCOM is a reactive shunt compensator belonging to the FACTS family. STATCOM is often used for voltage enhancement, power factor correction, and harmonics mitigation. The controller adjusts the injecting voltage to achieve the required compensation. This paper offers a Neuro-Fuzzy controller based on STATCOM to improve the unbalanced voltage in the distribution network. The paper shows the ability of the STATCOM to reduce the multiple effects of unbalanced voltage and dynamic loads together. The results show the ability of the new proposal to manage the load voltage up to 95% of the minimum value.

Keywords: STATCOM, FACTS, Vsc D-q Theory, Park Transformation, Neuro-Fuzzy, Unbalance Voltage, Fuzzy Logic Controller "FLC", Neuro-Fuzzy Logic Controller "NLFC", Artificial Neural Network "ANN".

ARTICLE INFORMATION

Author(s): Waseem Kh. Ibrahim, Mahmood T. Alkhayyat,

Mohammed Y. Suliman;

Received: 26/12/2024; Accepted: 07/08/2025; Published: 30/09/2025;

E-ISSN: 2347-470X; Paper Id: IJEER 2612-16; Citation: 10.37391/ijeer.130322

Webpage-link:

https://ijeer.forexjournal.co.in/archive/volume-13/ijeer-130322.html

Publisher's Note: FOREX Publication stays neutral with regard to jurisdictional claims in Published maps and institutional affiliations.

1. INTRODUCTION

Website: www.ijeer.forexjournal.co.in

STATCOM is a multifunctional device. The current quality is enhanced, and the flow of power is controlled by using STATCOM [1]. The equipment includes any device that uses semiconductor switches. These types of equipment mentioned negatively affected the power quality [2]. A heavy load immunizes the reactive power to be transmitted even with an essential voltage magnitude. Voltage fluctuation may cause hazardous effects on sensitive loads [8]. STATCOM is effective in regulating the current injected into the bus [3]. It serves various purposes, including compensating for voltage sags and swells, reducing line current harmonics, enhancing the power factor at the load, and providing compensation of reactive power in both the transmission line and the load. Additionally, STATCOM helps mitigate voltage fluctuations at the bus [4]. When paired with energy storage, STATCOM is particularly useful for controlling both the magnitude and phase angle of the injected voltage, with the Voltage Source Converter (VSC)

being used to manage the active and reactive power flow of the system [5].

2. VOLTAGE REGULATION AND COMPENSATION

The shunt device connections for the regulation of bus voltage are shown in figure 1. The model consists of a power line, a voltage source Vs, and a load. In the middle of the line, STATCOM injects the power. The phasor diagram shows that the line current angle has a relation with the load side, which means that the active component of the current IC is injected to enhance the line current Isc and then the load voltage. Figure 2 shows the Q-V characteristics of STATCOM, where it injects reactive power against an inductive load and enhances the bus voltage [6]. The near feeding of reactive power improves voltage regulation [7]. There are three approaches to improving voltage regulation: first, by utilizing a capacitor bank; second, through the use of a Voltage Source Inverter VSI [8]; and third, by implementing a Current Source Inverter CSI [9]. In figure 1, the current source device is employed to compensate for the reactive power of the load by either injecting or absorbing current IC from the network. This process enhances voltage regulation and reduces the reactive components in the source current. STATCOMs support the system during extreme conditions where the bus voltage may deviate significantly from the normal operating range of the compensator [10]. One of the primary benefits of using a Voltage Source Converter VSC is that it allows for the generation of reactive power without relying on capacitors, and it operates independently of the current [11].

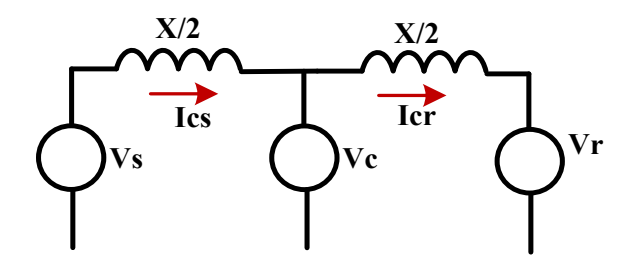
²Northern Technical University, Iraq; Email: m.t.alkhayyyat@ntu.edu.iq

³Northern Technical University, Iraq; Email: mohammed.yahya@ntu.edu.iq

^{*}Correspondence: Mahmood T. Alkhayyat, Email: m.t.alkhayyyat@ntu.edu.iq



Research Article | Volume 13, Issue 3 | Pages 572-579 | e-ISSN: 2347-470X



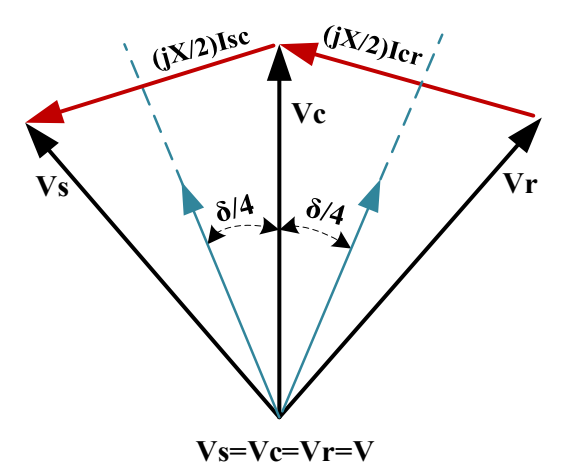


Figure 1. Principles of Shunt Compensation

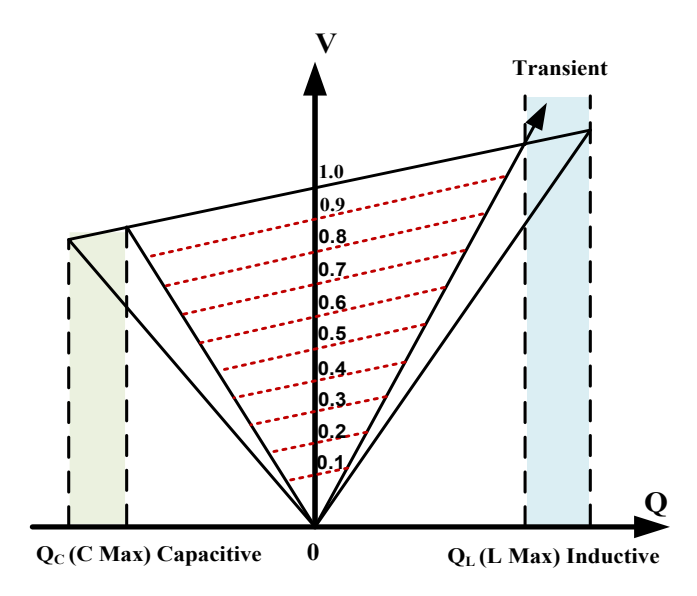


Figure 2. STATCOM V-Q characteristic

In the distribution system, the STATCOM connected before load as shown in *figure 3*.

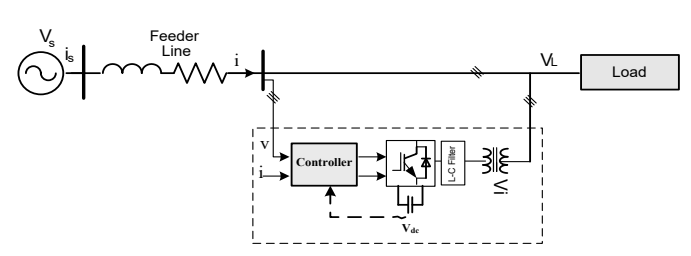


Figure 3. STATCOM connection

Website: www.ijeer.forexjournal.co.in

3. PV ENERGY SYSTEM MODEL

irradiance falling as well as its area affect the generated electric power from the PV energy system [12]. Optimal tilt angle is often used to increase the irradiance and consequently, the generated energy from the PV system. This optimal tilt angle is chosen to be equal to the latitude angle of the site [13]. The hourly generated power from the PV array can be determined by the following equation [14]:

$$P_{pv} = P_{rated} N_{pv} D_f \left(\frac{G}{G_{ref}} \right) \times \left(1 + K_T \left(\left(T_{amb} + G \left(\frac{NWCT - 20}{0.8} \right) \right) - T_{ref} \right) \right)$$

$$(1)$$

Where:

P_{PV}: PV produced power (kW) P_{rated}: Module output power (kW) N_{PV}: Number of PV modules D_f: PVderating factor (0.85)

G: Global utility fallen on the titled plane (kW/m2) $G_{\rm ref}$: Solar radiation at base conditions (1 kW/m2)

K_T: Peak power temperature coefficient

 T_{amb} : Ambient temperature ($^{\circ}$ C)

NWCT: Normal working cell temperature

Based on the status of the storage system, the photovoltaic (PV) conversion system can function in Maximum Power Point Tracking (MPPT) mode for optimal power extraction, or in off-MPPT mode to ensure power balance, as illustrated in *figures 4* and 5 [15]. Additionally, when there is an excess of power generation and the battery system has no available storage capacity, the energy management system transitions the PV controller from MPPT to off-MPPT mode to limit excess power generation and sustain power equilibrium in the off-grid system. [16].

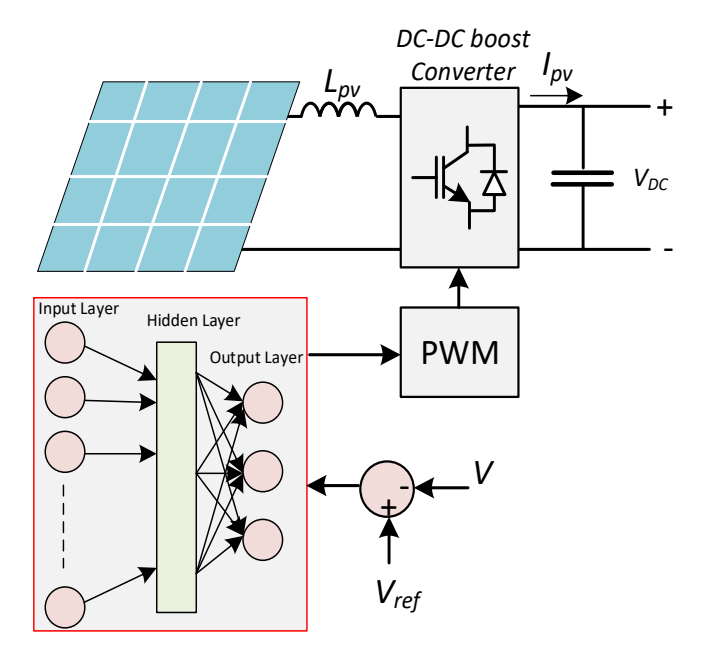


Figure 4. ANFIS PV-based DC supply controller



Research Article | Volume 13, Issue 3 | Pages 572-579 | e-ISSN: 2347-470X

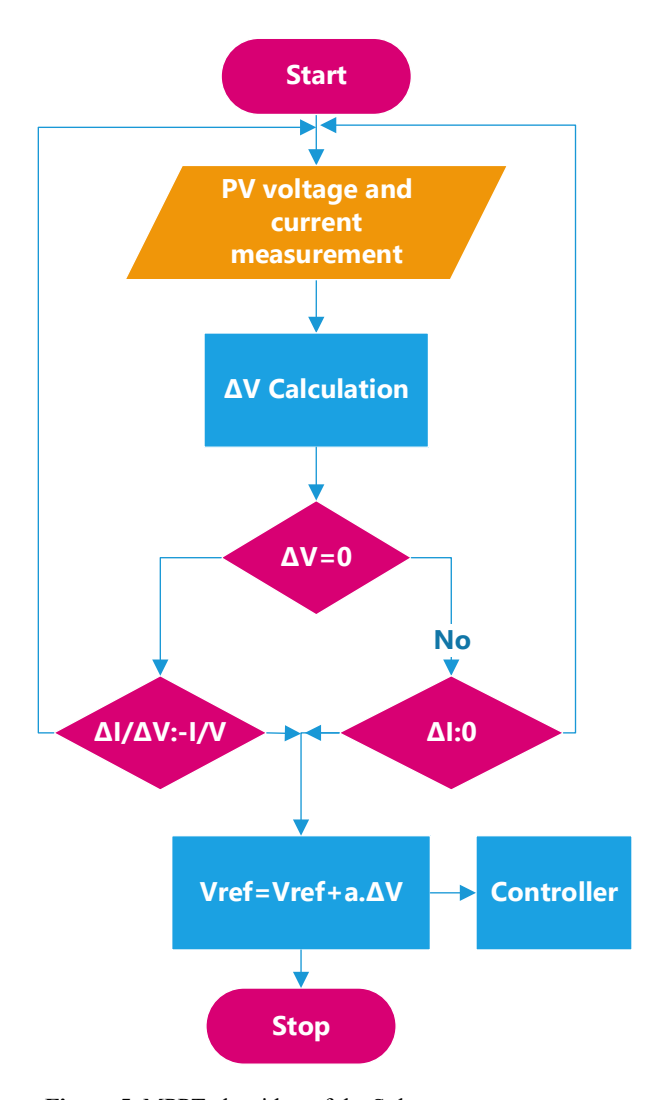


Figure 5. MPPT algorithm of the Solar energy system

4. MEASUREMENT OF REACTIVE POWER AND LINE VOLTAGE

The dq theory is applied to measure the voltages and reactive powers [17]. This theory can be used in both time and frequency domains. This feature makes dq applicable for different waveforms, thus designing a controller in real time [18]. Additionally, it is simple to differentiate between the mean value and the alternative value thanks to the straightforward transformation computations [19]. Dq philosophy involves a set of transformations, often referred to as the 'Park transformation,' which converts stationary coordinates (ABC) into rotating coordinates (dq) [20]. The application of dq theory, which involves variables such as v_a , v_b , and v_c , is explained as follows:

$$\begin{bmatrix} v_d \\ v_q \\ v_0 \end{bmatrix} = \frac{2}{3} \begin{bmatrix} \cos(\emptyset) & \cos(\emptyset - \frac{2\pi}{3}) & \cos(\emptyset + \frac{2\pi}{3}) \\ -\sin(\emptyset) & -\sin(\emptyset - \frac{2\pi}{3}) & -\sin(\emptyset + \frac{2\pi}{3}) \\ \frac{1}{2} & \frac{1}{2} & \frac{1}{2} \end{bmatrix} \begin{bmatrix} v_a \\ v_b \\ v_c \end{bmatrix}$$
(2)

$$\begin{bmatrix} i_d \\ i_q \\ i_0 \end{bmatrix} = \frac{2}{3} \begin{bmatrix} \cos(\emptyset) & \cos(\emptyset - \frac{2\pi}{3}) & \cos\left(\emptyset + \frac{2\pi}{3}\right) \\ -\sin(\emptyset) & -\sin\left(\emptyset - \frac{2\pi}{3}\right) & -\sin(\emptyset + \frac{2\pi}{3}) \\ \frac{1}{2} & \frac{1}{2} & \frac{1}{2} \end{bmatrix} \begin{bmatrix} i_a \\ i_b \\ i_c \end{bmatrix}$$
(3)

$$\emptyset = (\omega t + \theta) \tag{4}$$

Where " ϕ " signifies the phase difference angle between secure and gyrating coordinates over time, and " θ " epitomizes the angle formed by voltage and current. The remunerated active and reactive power:

$$P = V_d I_d + V_q I_q \tag{5}$$

$$Q = V_d I_q \cdot V_q I_d \tag{6}$$

The cumulative voltage is:

$$V = \sqrt{(V_d^2 + V_q^2)} \tag{7}$$

5. DESIGN OF STATCOM CONTROL SYSTEM

The STATCOM's control system block diagram is depicted in figure 4. To eliminate the high-frequency component, the signals are passed over a low-pass filter, and next, the phase voltages are measured. Equations 3 and 4 use "park transformation" to calculate the dq components. The accumulated voltage is then calculated using eq. 8 and fed back into the closed-loop control system, where it is equated to the busbar's "Vref" customary point orientation voltage to generate error signals "Verror".

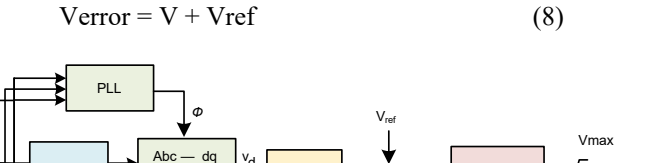


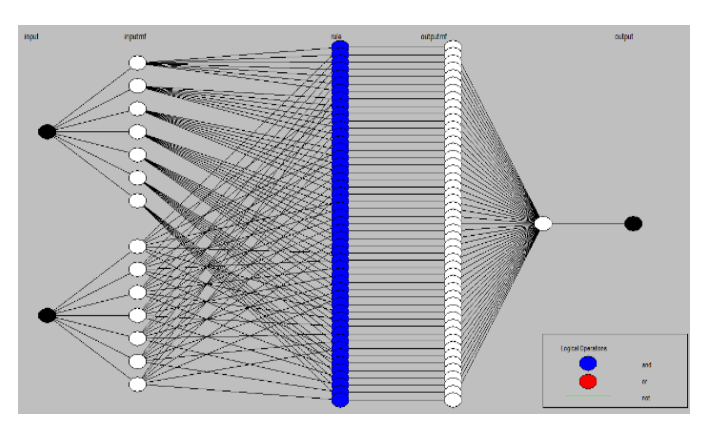
Figure 6. Block Diagram of System Control

6. CONTROL SYSTEM BASED ON FUZZY-LOGIC

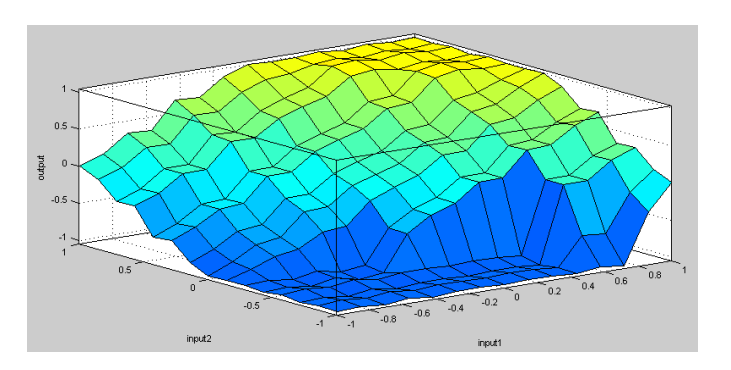
FLC was used in this study; it is suitable for schemes with difficult-to-deduce mathematical models [21]. This study uses the Takagi-Sugeno inference mechanism systems [22]. Takagi-Sugeno's "membership functions" are tuned using an "ANN" [23]. For the FLC that can use ANN adaptive erudition, training can be easier, and the fuzzy rule base is reduced. [24]. A fuzzy system is made up of five layers, each with two types of parameters, some of which must be tuned while others do not during the training process. Refer to [25] for more information on mimicking FLC design procedures for output in five layers. The discourse universe is divided into 5 triangle MFs with a 50% overlap. The controller's input is error and Δ error, subsequent in 25 control rules based on linear functions as made known in

Research Article | Volume 13, Issue 3 | Pages 572-579 | e-ISSN: 2347-470X

figures 7(a) and 7(b). Tuning these rules with ANN, two clusters of facts are used. *Verror* and $\Delta Verror$ are two input vectors, and the harvest is the intonation catalog "m".



(a) fuzzification



(b) surface validation **Figure 7.** NF theory

7. SIMULATION AND RESULTS

The proposed system prototype consists of the feeder with load branches in steps of 14MW, 28MW, and 32MW. This means the load change is in the range of 1, 2, and 2.28 p.u. respectively. The supply is provided by two sources: the main grid supply with PV energy, with 28MW in power variable depending on the irradiance and temperature of PV operation, as shown in figure 8. Solar energy with a time interval from 6 am to 6 pm, as shown in figure 9. The adaptive Neoro-Fuzzy controller is programmed to control STATCOM to the injection voltage as designed before. The proposed model is shown in Figure 10. To validate the Neoro-Fuzzy controller sudden step change in load with unbalanced conditions as shown in figures 11 and 12 for load voltage and load current respectively. Figure 13 the sudden unbalanced load occurs at time 0.2 seconds, the unbalanced load made to actions decrease in a voltage drop of 20% and also distortion in the voltage waveform, in addition increase in load current, at time 0.4-second STATCOM responded to the situation of the load condition. The time is calculated based on 24 hours (60*60*24) for solar energy durations. The study model consists of a feeder and two load branches with variable loads for balance and an extra load for unbalanced situations. The STATCOM on the load side is responsible for

compensating the load voltage. The model is tested by varying the unbalanced load and continuously measuring the voltage at the load bus for compensation, as shown in figure 11. The unbalanced load enters at t=0.2 Seconds, the voltage drops by about 20% of the nominal value, also the load currents increase as shown in figure 12. The action of STATCOM is done at t=0.40 seconds to compensate for the unbalanced voltage, as shown in figure 13. Also, the load current was modified as publicized in figure 14. The STATCOM compensated voltage is publicized in figure 15. Figure 16 portrays the relationship between load voltage and STATCOM voltage. As the load increased, the result presented that the load voltage drop increased proportionately. The maximum drop (0.2 pu) occurred between 0.20 and 0.40 seconds, respectively. The system's reaction to a stage change in the load voltage in a capacitive manner (forward manner) is depicted in figure 17. Inductive style, where the voltage leads the line current, was used to accomplish the opposite. According to the results, the "NFLC" that was designed responds more quickly, smoothly, and with less oscillation. The p-v curve is displayed in figure 17, and the results indicate that the system voltage with STATCOM increased the stability margin and amplitude by roughly 20%.

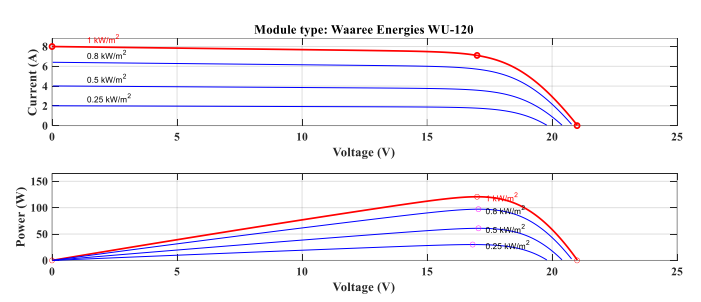


Figure 8. PV Operating Point

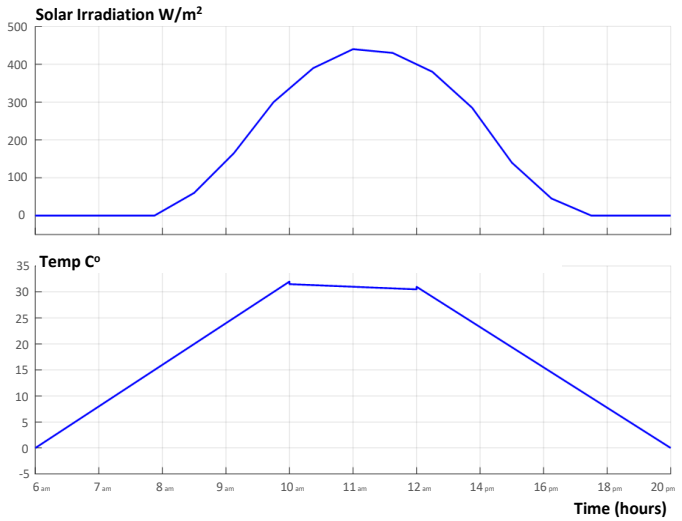


Figure 9. Irradiance versus temperature for PV energy

The load current earlier and the next compensation are displayed in *figure 9*. It is evident from the results of the power-voltage characteristic in *figure 12* that the load voltage enlarged the amplitude with STATCOM while also amplifying the constancy boundary.



Research Article | Volume 13, Issue 3 | Pages 572-579 | e-ISSN: 2347-470X

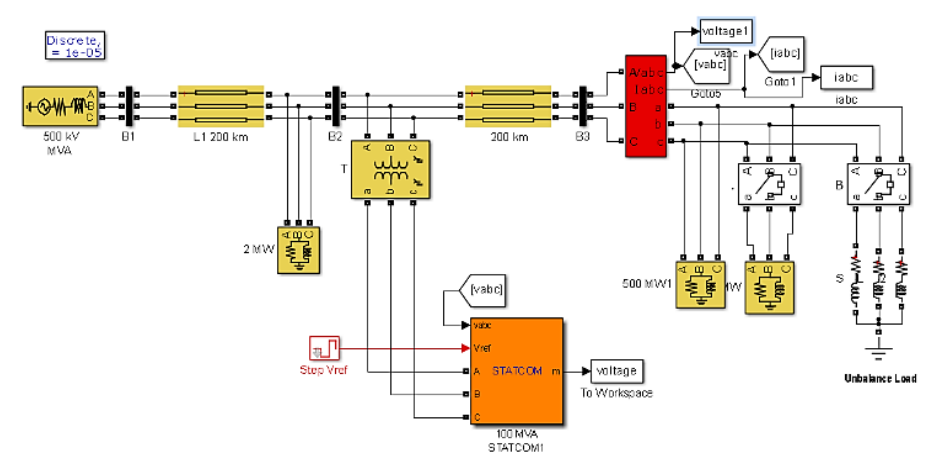


Figure 10. The Simulation System Model

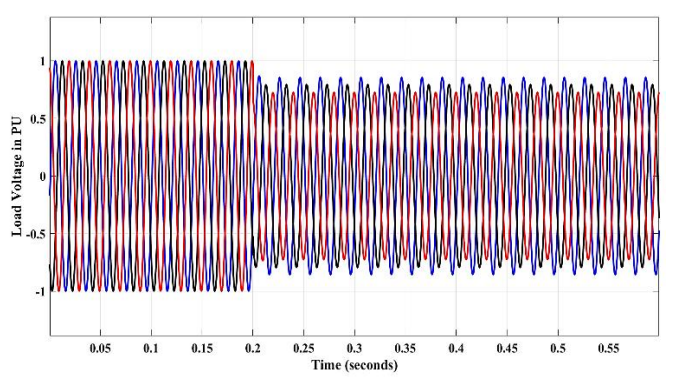


Figure 11. Three-phase voltage waveforms load

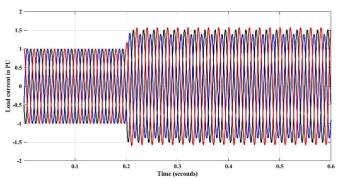


Figure 12. Three-phase current waveforms load

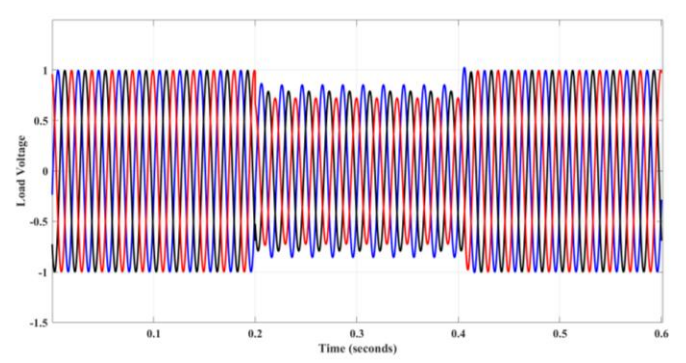


Figure 13. Fourier analysis of inverter output

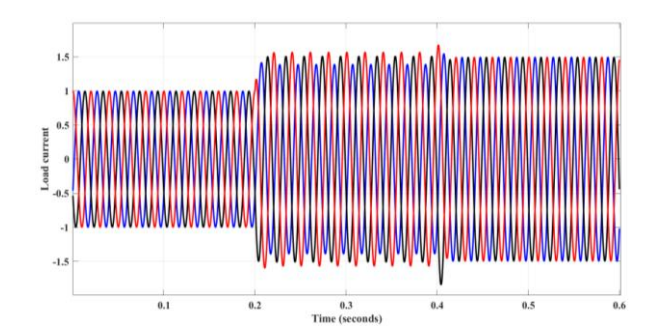


Figure 14. Load current

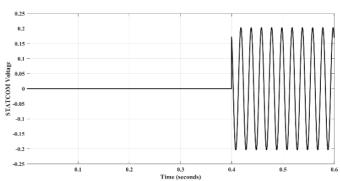


Figure 15. The STATCOM Voltage

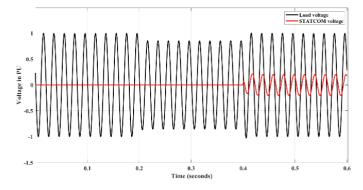
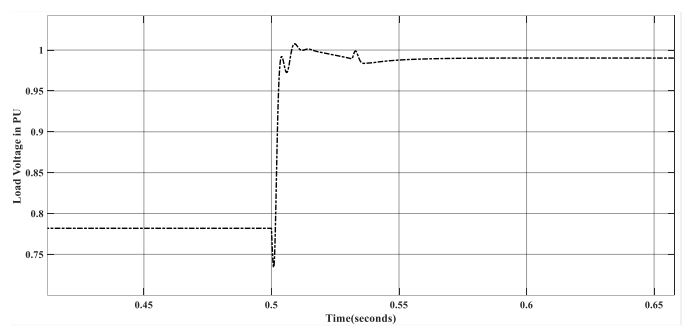


Figure 16. The load voltage verses STATCOM voltage

Research Article | Volume 13, Issue 3 | Pages 572-579 | e-ISSN: 2347-470X



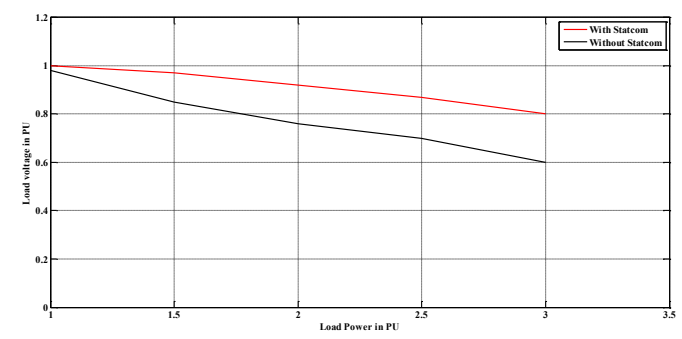


Figure 17. Voltage response using STATCOM

Figure 18. The PV Curve

STATCOM can also reduce the effect of dynamic load. *Figure 19* shows the system including passive and dynamic loads. The main dynamic loads represented in the real world are the rotating machines. On the other hand, the most effective dynamic loads occur during starting. *Figures 20, 21,* and 22 show the effect of STATCOM for reducing the swing in powers and unbalanced voltage, respectively, caused by dynamic loads.

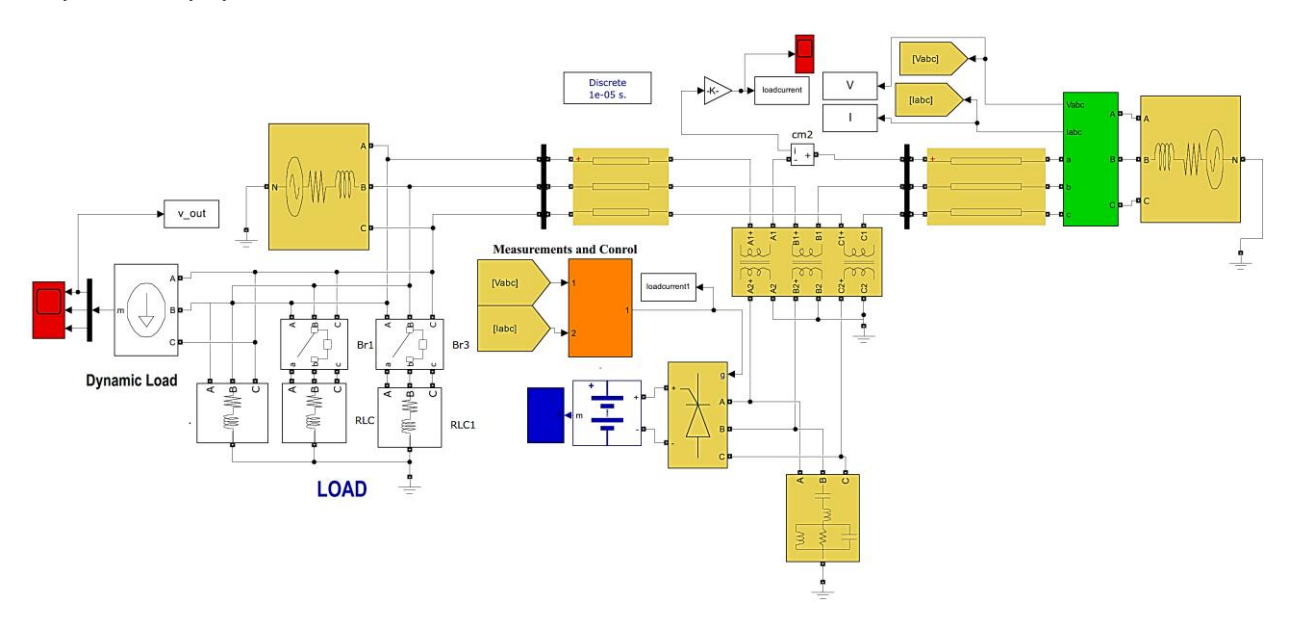


Figure 19. Power system including dynamic load

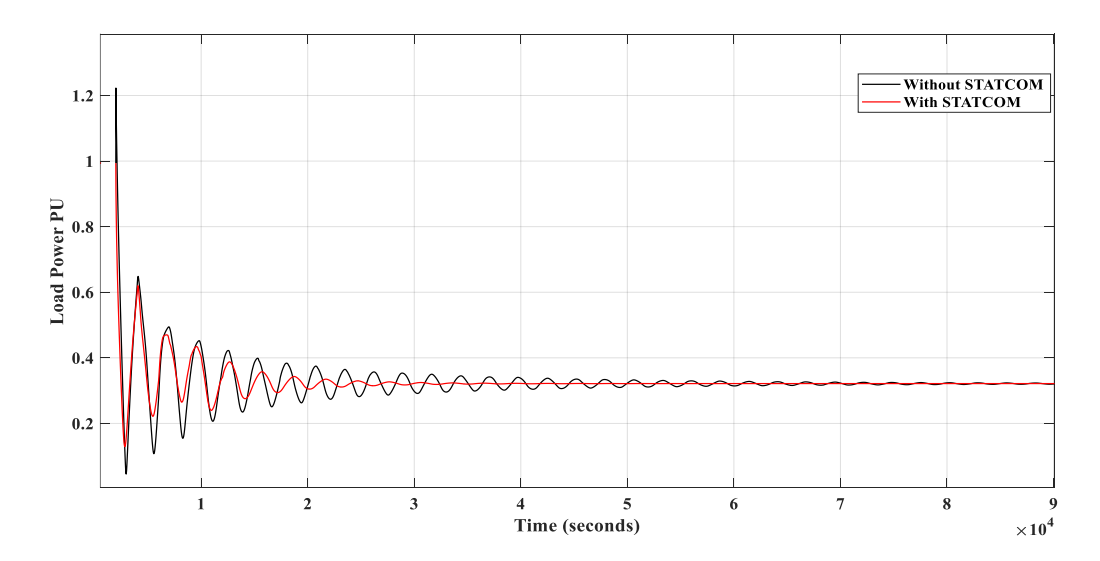


Figure 20. Power swing enhancement with STATCOM

Research Article | Volume 13, Issue 3 | Pages 572-579 | e-ISSN: 2347-470X

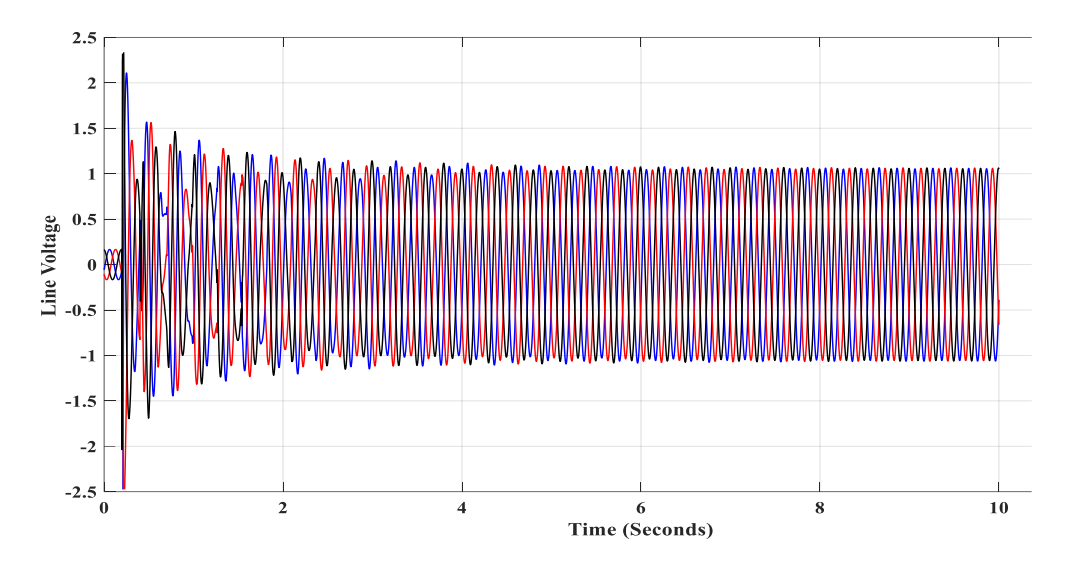


Figure 21. Starting dynamic load

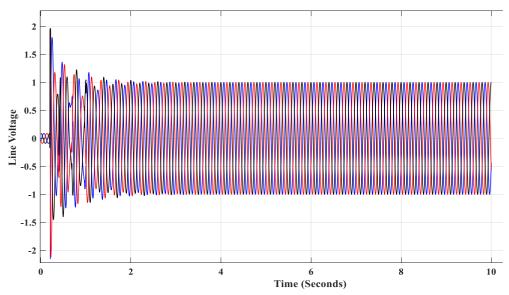


Figure 22. Starting dynamic load with STATCOM

CONCLUSION

In this paper, an FLC enhancing STATCOM performance has been designed and implemented in the location of load-side conditions. Many Incidents of unbalanced load disturbances have been focused on utilizing the modeling MATLAB/SIMULINK. Simulation results illustrated the compensation designed system-based FLC with ANN, enhancing the voltage of the load bus and increasing the margin of stability. The model simulation compared the injected voltage for compensation both after and before was focusing on two types of unbalanced load and balance cases. In both statements, the designed STATCOM is adequate for restoring the bus voltage amplitude of the demand load side to its nominal level of about 95%. Additionally, the fast response of the designed controller in compensating for load side conditions, especially at unbalanced loads, is achieved within a few milliseconds, which is less than one cycle. This is very important for real-time implementation. STATCOM can

enhance the swing in power as well as in voltage by reducing the effect of multiple voltage unbalanced and dynamic loads together.

REFERENCES

- E. Acha, C. Fuerte, H. Ambriz, C. Angeles-Camacho, "FACTS Modeling and Simulation in Power Networks", *John Wiley & Sons Ltd*, 2004, pp. 21-23.
- [2] Alkhayyat, M.T., Suliman, M.Y., Adaptive Neuro-Fuzzy Controller Based STATCOM for Reactive Power Compensator in Distribution Grid, 2022, PRZEGLĄD ELEKTROTECHNICZNY R. 98(NR 4/2022) p, p.107-112,2022, DOI: 10.15199/48.2022.04.23.
- [3] Hingorani and L. Gyugyi, "Understanding FACTS, Concepts and technology of flexible AC transmission systems", *IEEE Press*, 2000, pp. 172-174.
- [4] Mahmood T. Alkhayyat, Mohammed Yahya Suliman, Faisal Aiwa, PQ & DQ Based Shunt Active Power Filter with PWM & Hysteresis Techniques, PRZEGLĄD ELEKTROTECHNICZNY, ISSN 0033-2097 R. 97 NR 9/2021, 2021, DOI: 10.15199/48.2021.09.17



Research Article | Volume 13, Issue 3 | Pages 572-579 | e-ISSN: 2347-470X

- [5] Suliman, M.Y., Farrag, M.E., Bashi, S., Design of fast real time controller for the SSSC based on takagi-sugeno (TS) adaptive neuro-fuzzy control system, Renewable Energy and Power Quality Journal, 1(12), 2014, pp. 1025-1030,575. DOI:10.24084/repqj12.575
- [6] Alkhayyat, M.T., Sinan M. Bashi, Reduce the Impact of Voltage Sag with Phase Jumping in AC Line Using Unified Power Quality Conditioners UPQC and Open UPQC, 2nd International Conference on Electrical, Communication, Computer, Power and Control Engineering, ICECCPCE, 2019, pp. 114-119, DOI: 10.1109/ICECCPCE46549.2019.203758
- [7] Liu Qing and Wang Zengzing, "Coordinated design of multiple FACTS controllers based on fuzzy immune coevolutionary Algorithm", *IEEE Power & Energy Society General Meeting* , Calgary, AB, , 2009, pp. 1-6.
- [8] Alkhayyat, M.T., Suliman, M.Y., Neuro Fuzzy based SSSC for Active and Reactive Power Control in AC Lines with Reduced Oscillation, 2021, PRZEGLAD ELEKTROTECHNICZNY, 2021, 1(3), pp.77-81.
- [9] Ali, A.J., Suliman, M.Y., Khalaf, L.A., Sultan, N.S., Performance investigation of stand-alone induction generator based on STATCOM for wind power application, International Journal of Electrical and Computer Engineering, 2020, 10(6), pp. 5570-5578.
- [10] Alkhayyat, M.T., Suliman, M.Y., Neuro Fuzzy based SSSC for Active and Reactive Power Control in AC Lines with Reduced Oscillation, 2021, PRZEGLĄD ELEKTROTECHNICZNY, 2021, 1(3), pp.77-81.
- [11] V. Ponananthi and B. Rajesh Kumar, "Three-phase statcom controller using D-Q frame theory for a three-phase SEIG feeding single phase loads", Electronics and Communication Systems (ICECS), 2nd International Conference IEEE Conference, Coimbatore, India, , 2015, 2015,26-27 Feb., pp.926-931.
- [12] Alkhayyat, M.T., Khalaf, L.A., Suliman, M.Y., Adaptive Control for Power Management Based on Renewable Energy, 2023PRZEGLĄD ELEKTROTECHNICZNY 2023, 1(12), pp. 104-108, DOI: 10.15199/48.2023.12.19
- [13] Antar, R.K., Suliman, M.Y., Saleh, A.A., Harmonics resonance elimination technique using active static compensation circuit, Bulletin of Electrical Engineering and Informatics, 2021, 10(5), pp. 2405-2413.
- [14] Suliman, M.Y., Bashi, S.M., Fast response SSSC based on instantaneous power theory, 2013 International Conference on Electrical, Communication, Computer, Power, and Control Engineering, ICECCPCE 2013, 2014, pp.174-178, 6998757.
- [15] Ogunboyo P. Taiwo, Remy T and Innocent E. Davidson," Voltage profile enhancement in low voltage 11/0.4 kV electric power distribution network using dynamic voltage restorer under three phase balance load", 2017, IEEE AFRICON conference, pp 991-996.
- [16] P. T Ogunboyo, R. Tiako, I. E. Davidson, Application of Dynamic Voltage Restorer for Power Quality Improvement in Low Voltage Electrical Power Distribution Network: An Overview, International Journal of Engineering Research in Africa. ,2017, 28, 143-156.
- [17] Damon Bazargan, Behrooz Bahrani and Shaahin Filizadeh," Reduced Capacitance Battery Storage DC-Link Voltage Regulation and Dynamic Improvement Using a Feedforward Control Strategy", IEEE Transactions on Energy Conversion, vol 33, no. 4, pp 1659-1668, 2018.
- [18]C. Ren, X. Han, L. Wang, Y. Yang, w. qin, and P. Wang, "High performance three-phase pwm converter with reduced dc-link capacitor under unbalanced ac voltage conditions," IEEE Transactions on IndustrialElectronics,, 2017, vol. PP, no.99, pp. 1–1.
- [19] X. Guo, W. Liu, X. Zhang, X. Sun, Z. Lu, and J. M. Guerrero, "Flexible control strategy for grid-connected inverter under unbalanced grid faults without PLL," IEEE Trans. Power Electron., 2015, vol. 30, no. 4, pp. 1773-1778, Apr. 2015.
- [20]H. B. Tolabi, M. H. Ali, and M. Rizwan, "Simultaneous reconfiguration, optimal placement of DSTATCOM and photovoltaic array in distribution system based on fuzzy ACO approach," IEEE Trans. Sustain. Energy, 2015, vol. 6, no. 1, pp. 210–218, Jan. 2015.

Website: www.ijeer.forexjournal.co.in

- [21]T. Yuvraj, K. Ravi, and K. R. Devabalaji, "DSTATCOM allocation in distribution networks considering load variation using bat algorithm," Ain Shams Eng. J., 2015.
- [22] P. Dash, M. Mangaraj, and T. Penthia, "Mid-point capacitor type VSC based DSTATCOM with a supercapacitor for power quality improvement under unbalanced loading condition" IEEE Student's Conference on SCEECS., Mar. 2016.
- [23] Suliman, M.Y., Alkhayyat, M.T., High impedance fault detection in radial distribution network using discrete wavelet transform technique, Archives of Electrical Engineering, 70(4), 2021, pp. 873-886, 2021.
- [24] Alkhayyat, M.T., Aiwa, F., Alhafidh, A.S., Suliman, M.Y., Power Transformer Inrush Current Minimization During Energization using ANFIS based Peak Voltage Tracking Approach, *International Journal of Electrical and Electronics Research*, 2024, 12(1), pp. 211–218, DOI: 10.37391/IJEER.120130
- [25] W. L. Chen and J. S. Lin, "One-dimensional optimization for proportional-resonant controller design against the change in source impedance and solar irradiation in PV systems," IEEE Trans. Ind Electron., 2014, vol. 61, no. 4, pp. 1845-1854.



© 2025 by Hussein Shakor Mogheer, Alrubei Mohammed A.T., Yassir AL-Karawi. Submitted for possible open access publication under the terms and

conditions of the Creative Commons Attribution (CC BY) license (http://creativecommons.org/licenses/by/4.0/).